Combining Self-Phase Modulation and Optimum Modulation Conditions to Improve the Performance of 10-Gb/s Transmission Systems Using MQW Mach–Zehnder Modulators

J. C. Cartledge, *Senior Member, IEEE, Member, OSA*

***Abstract*—For 10-Gb/s transmission over nondispersion shifted fiber, the combined use of self-phase modulation (SPM) and joint optimization of the bias and modulation voltages to increase the dispersion limited transmission distance is considered for multiple quantum well Mach–Zehnder modulators. For the dual drive (push-pull) modulation format, the dependence of the receiver sensitivity on fiber length and average transmitted optical power is determined for both conventional and π phase-shift modulators with either symmetric or asymmetric Y-branch waveguides. When SPM is negligible and the optical extinction ratio is maximized, the modulator design must be considered carefully in order to increase the transmission distance. By combining SPM and optimum modulation conditions, the dependence of the system performance on the modulator design is reduced substantially. For an average transmitted optical power of 12.5 dBm, the receiver sensitivity for transmission over 140 km of fiber varies by only 0.3 dB for the different modulator designs. This compares with a variation of 3.1 dB for maximum extinction ratio modulation.**

***Index Terms*—Modulator chirp, multiple quantum-well (MQW) Mach–Zehnder optical modulator, optical communications, transmission system performance.**

I. Introduction

MULTIPLE quantum-well (MQW) Mach–Zehnder modulators have the attractive feature that the chirp of the transmitted signal is a function of the material composition of the modulator waveguide, the splitting ratios of the two Y-branch waveguides, the differential length between the two arms of the interferometer, and the modulating voltages applied to each arm of the modulator [1]–[13]. Considerable effort has been placed on optimizing the negative chirp properties of MQW Mach–Zehnder modulators in order to maximize the transmission distance in the presence of group velocity dispersion (GVD). This optimization, in terms of the composition of the MQW active layer and the device structure, is aimed at obtaining an appropriate amount of negative chirp and a high extinction ratio. A result of this effort is the π phase-shift Mach–Zehnder modulator with asymmetric Y-branch waveguides [7]. A differential length of half a wavelength between the two arms of the modulator leads to a phase shift of π radians between the optical signals at the output Y-branch. The asymmetric Y-branch waveguides lead to a greater proportion of the incident optical signal in the arm that contributes negative chirp to the modulated optical signal and has greater absorption in the on-state.

With negative chirp, the optical carrier frequency decreases during the leading edge of a pulse and increases during the trailing edge. The GVD of standard single mode fiber at a wavelength of 1.55 μm causes a negatively chirped pulse to compress as it propagates along the fiber. With the appropriate amount of negative chirp, the system reach can be increased relative to that of the chirp-free case. When a booster amplifier is used, the transmitted optical power can be increased to the point where self-phase modulation (SPM) due to the Kerr nonlinearity in single mode fiber becomes important. In this case, the refractive index of the fiber depends on the intensity of the optical signal. The transmitted signal induces a modulation dependent variation in the refractive index, which in turn induces a modulation dependent variation in the phase of the optical signal. This phase modulation contributes further to the negative chirp of the transmitted signal and can be beneficial in reducing the impact of the phase distortion arising from GVD. Hence, SPM can yield an increase in the transmission distance compared to that achieved when nonlinear effects are negligible and GVD is the dominant cause of signal distortion. Results for electroabsorption modulators have shown that the implications of SPM on system performance strongly depend on the precise nature of the modulator chirp [14].

For MQW Mach–Zehnder modulators and electroabsorption modulators, the bias and modulation voltages can be optimized to yield the minimum degradation in receiver sensitivity for a given fiber length [14], [15]. The system reach can be increased relative to that obtained with the modulation conditions that yield the maximum extinction ratio. This optimization is aimed at finding an appropriate compromise between the extinction ratio and chirp of the transmitted optical signal.

In this paper, the combined use of SPM and optimum modulation conditions is assessed for conventional MQW Mach–Zehnder modulators and π phase-shift Mach–Zehnder modulators. For 10 Gb/s transmission over nondispersion shifted fiber, the system performance is evaluated for modulators with symmetric and asymmetric Y-branch waveguides.

Manuscript received April 9, 1999; revised January 5, 2000. This work was supported by Communications and Information Technology Ontario and by the Natural Sciences and Engineering Research Council of Canada.

The author is with the Department of Electrical and Computer Engineering, Queen's University, Kingston, ON, K7L 3N6 Canada.

Publisher Item Identifier S 0733-8724(00)03743-9.

The results provide a comprehensive assessment of the impact that the modulator structure has on receiver sensitivity.

II. System Performance Evaluation

The MQW Mach–Zehnder modulator consists of an input Y-branch splitter, two arms with independent drive electrodes, and an output Y-branch combiner. The CW optical signal incident on the input Y-branch is split into the two arms of the interferometer. The on-state is achieved when there is no differential phase shift between the two signals at the output Y-branch and the off-state is achieved when there is a differential phase shift of π radians. The output signal from the modulator is, to a good approximation, the sum of the fields at the outputs of the two arms. For a modulator with the same input and output Y-branch splitting ratios, this signal is given by

$$\begin{aligned} E(V_1, V_2) &= \frac{E_0}{1+SR}\left[SR\exp\left(-\left(\frac{\Delta\alpha_a(V_1)}{2}+j\Delta\beta(V_1)\right)L\right)\right. \\ &\quad \left.+\exp\left(-\left(\frac{\Delta\alpha_a(V_2)}{2}+j\Delta\beta(V_2)\right)L-j\phi_0\right)\right] \\ &\equiv \sqrt{I(V_1, V_2)}\exp(j\Phi(V_1, V_2)) \end{aligned} \tag{1}$$

where

$SR = P_1/P_2$	Y-branch power splitting ratio;
$\Delta\alpha_a/2$	attenuation constant;
$\Delta\beta$	phase constant;
L	interaction length of the modulator arm;
ϕ_0	0 radians for a conventional modulator and π radians for a π phase-shift modulator;
V_1 and V_2	voltages applied to arms 1 and 2, respectively;
I	intensity of the optical signal;
Φ	phase.

For $i = 1, 2$

$$V_i(t) = V_{bi} + V_{\mathrm{mod}\,i}\,v(t) \tag{2}$$

where

V_{bi}	bias voltage;
$V_{\mathrm{mod}\,i}$	peak-to-peak modulation voltage;
$v(t)$	modulation waveform with a peak-to-peak amplitude of one and an average value of zero.

The dependence of the attenuation and phase constants on the applied voltage can be obtained either by direct measurement of a straight section of waveguide cut from one arm of a modulator [16] or by using the cosine rule and measurements of the voltage dependence of the intensity of the output signal for each arm with the other arm strongly absorbing [17]. As illustrated in Fig. 1 for a 600-μm-long waveguide, the absorption (and hence $\Delta\alpha_a$) and the change in phase $\Delta\beta$ are nonlinear functions of the applied voltage. The strip-loaded waveguide consists of a 2.0-μm-thick p-type InP layer, an MQW intrinsic region composed of twenty InGaAsP wells and InP barriers, and a 2.1-μm-thick n-type InP layer. The wells and barriers are 100 Å thick [1].

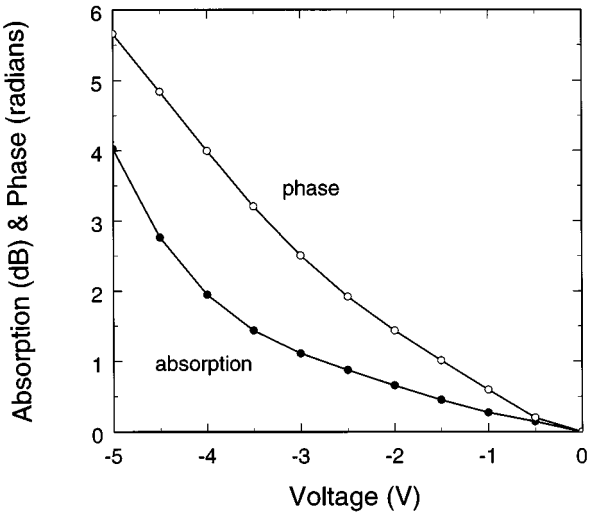

Fig. 1. Dependence of the absorption and phase of the optical signal on applied voltage for each arm of a π phase-shift modulator with a splitting ratio of 1.3.

The small-signal α-parameter, which quantifies the modulator chirp, is given by [18]

$$\alpha(V_1, V_2) = 2\frac{d\Phi(V_1, V_2)}{d(\ln(I(V_1, V_2)))}$$

and can be determined numerically from (1). The calculation of the α-parameter depends on the incremental changes in V_1 and V_2 and hence the modulation format. Dual drive (push–pull) modulation ($\Delta V_1 = -\Delta V_2$) and single drive modulation ($\Delta V_1 \neq 0$ and $\Delta V_2 = 0$) are used most frequently.

To comprehensively assess the implications of the combined use of SPM and optimum modulation conditions on system performance, the modulator model (1) is implemented in a simulation program which includes measured frequency responses for system components, fiber group velocity dispersion, the Kerr nonlinearity, receiver noise, and optimization of the decision point. The drive voltages $V_1(t)$ and $V_2(t)$ are obtained by filtering a nonreturn-to-zero (NRZ), 128-bit pseudorandom binary sequence (PRBS) waveform using the measured frequency response of a modulator.[1] The prefiltered waveform is based on a trapezoidal pulse with rise- and fall-times (10–90%) of 32.5 ps. The modulated optical signal is obtained using (1). The Schrödinger equation, which describes the propagation of the modulated signal over an optical fiber, is solved using the split-step Fourier technique. The detected photocurrent at the receiver is filtered using measured frequency responses for a p-i-n photodiode–preamplifier module, baseband amplifiers and low-pass filter. The receiver noise, which includes circuit noise and shot noise, is considered semi-analytically by combining sampled values of the output signal from the receiver with the assumption of Gaussian distributed noise. For a given fiber length, the receiver sensitivity is determined by evaluating the bit-error ratio (BER) as the strength of the optical signal is

[1]The 128-bit PRBS differs from the 2^7-1 PRBS found on pattern generators by the addition of a "0" bit; the "0000000" sequence that is excluded in a hardware implementation appears in a periodic repetition of the 128-bit PRBS. When using the fast Fourier transform (FFT), it is beneficial to have an even number of bits.

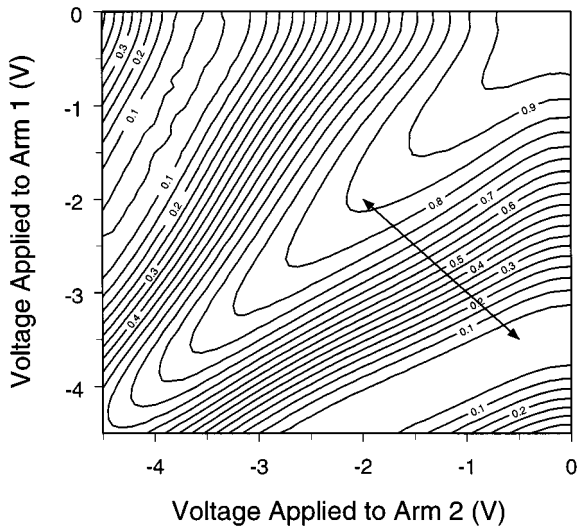

Fig. 2. Transmission contour for a conventional Mach–Zehnder modulator with Y-branch splitting ratios of 0.75.

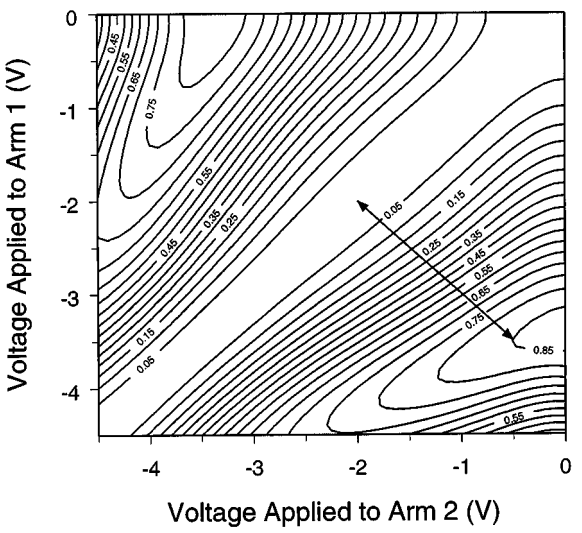

Fig. 3. Transmission contour for a π phase-shift Mach–Zehnder modulator with Y-branch splitting ratios of 1.3.

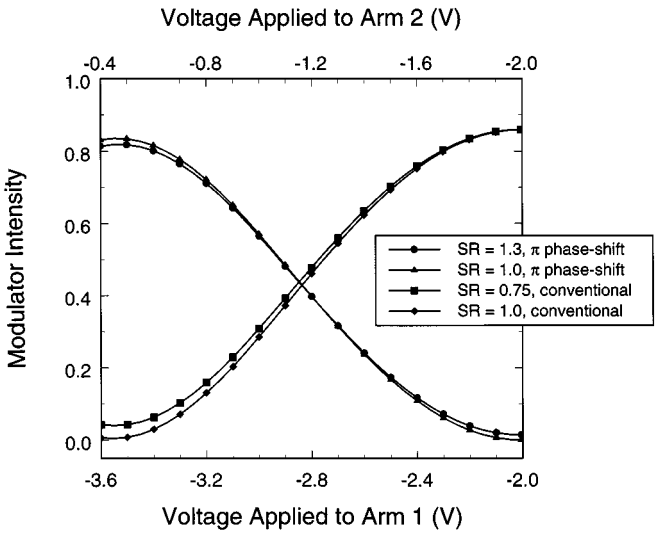

Fig. 4. Transmission curves as a function of the applied voltages that yield push–pull operation for four modulators.

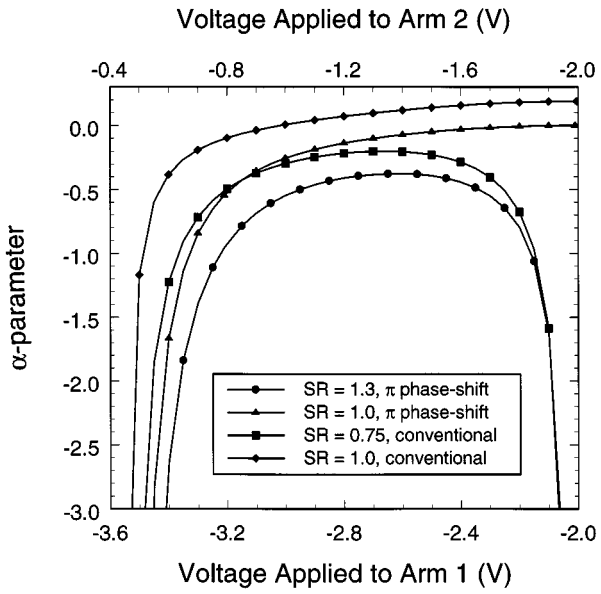

Fig. 5. Dependence of the α-parameter on the applied voltages that yield push–pull operation for four modulators.

varied at the receiver. The threshold level and sampling time are jointly optimized under a minimum BER criterion.

III. Results

The implications of optimizing the bias and modulation voltages for different transmitted powers are considered for four different modulator designs; conventional modulators with Y-branch splitting ratios of 1 and 0.75, and π phase-shift modulators with splitting ratios of 1 and 1.3. While the data in Fig. 1 is for a specific π phase-shift modulator, it is also used for the other modulator designs as this allows direct comparison of the results. It should be noted that the data describes the waveguide properties independently of the Y-branch splitting ratios and differential length between the arms of the modulator. For push–pull modulation, the optical signals in the two arms experience phase changes of different magnitudes and opposite signs as the modulator is switched from the off-state to the on-state. By using asymmetric Y-branches to direct more power into the arm with a positive phase change ($SR < 1$ for the conventional modulator, $SR > 1$ for the π phase-shift modulator), the negative chirp properties of the modulator are enhanced. When the effects of fiber nonlinearities are negligible, an increase in the dispersion limited transmission distance is obtained for asymmetric Y-branch waveguides [3], [7], [10].

Using the results in Fig. 1 and (1), contour plots of the output signal for a conventional modulator with a Y-branch splitting ratio of 0.75 and a π phase-shift modulator with a splitting ratio of 1.3 are illustrated in Figs. 2 and 3, respectively. The conventional modulator is in the on-state when the voltages applied to the two arm electrodes are equal. Due to the differential length between the two arms of the interferometer, the π

TABLE I
PARAMETER VALUES FOR 10 Gb/s SYSTEM PERFORMANCE EVALUATION

Parameter	*Value*
Fiber attenuation	0.2 dB/km
Dispersion coefficient (1550 nm)	17 ps/(km-nm)
Zero dispersion wavelength	1312 nm
Nonlinear coefficient	2.31×10^{-20} m^2/W
Effective area (1550 nm)	80 μm^2
Wavelength	1557 nm
Photodiode responsivity	1.0 A/W
Photodiode dark current	10 nA
Equivalent input noise current	15 pA/$\sqrt{\text{Hz}}$

phase-shift modulator is in the off-state under these drive conditions. The straight line in each of the plots depicts the dual drive (push–pull) mode of operation considered here. The normalized intensity of the optical signal ($|E(V_1, V_2)/E_0|^2$) along this line ($V_{b1} + V_{b2} = -4$ V) is illustrated in Fig. 4 for each of the four modulators. Due to the absorption that occurs in each arm of the modulator, the peak value of the normalized intensity is less than one and the π phase-shift modulator with a splitting ratio of one exhibits the greatest extinction in the off-state.

The dependence of the α-parameter on applied voltage is shown in Fig. 5. The curves exhibit two distinct types of behavior. For the π phase-shift modulator with a splitting ratio of 1.3 and the conventional modulator with a splitting ratio of 0.75, the α-parameter increases to a value of -0.5 and -0.3, respectively, and then decreases as the modulator is switched from the off-state to the on-state. For a splitting ratio of 1, the α-parameter of the π phase-shift (conventional) modulator decreases monotonically from (increases monotonically toward, respectively) a value of about "0" as the modulator is switched from the off-state to the on-state. For the conventional modulator with a splitting ratio of 1, the α-parameter is positive for $V_1 > -3$ V ($V_2 < -1$ V).

An alternative way to distinguish the chirp properties of the four Mach–Zehnder modulators is to use an effective transmission system performance α-parameter [19]. For the data in Fig. 1 and 100 km transmission, the transmission performance α-parameter is -0.3 for a π phase-shift modulator with a splitting ratio of 1; -1 for a π phase-shift modulator with a splitting ratio of 1.3; -0.15 for a conventional modulator with a splitting ratio of 1; and -0.6 for a conventional modulator with a splitting ratio of 0.75.

The parameter values used to obtain the numerical results are given in Table I. The measured frequency responses for the modulator and receiver (p-i-n photodiode–preamplifier module and baseband amplifiers) are illustrated in Fig. 6. The 3 dB bandwidths of the modulator and receiver are 11.1 and 6.6 GHz, respectively. The dependence of the receiver sensitivity (for a bit error ratio of 10^{-9}) on fiber length is illustrated in Fig. 7 for a conventional modulator with a splitting ratio of 1. Results are presented for the case of maximum extinction ratio (ER) modulation ($V_{b1} = -2.75$, $V_{b2} = -1.25$, and $V_{\text{mod}\,1,2} = 1.5$ V) and for optimized modulation. In the latter case, the bias and modulation voltages are jointly optimized to yield the best receiver sensitivity for each fiber length. In order to focus on the performance implications of the modulator, the average transmitted optical power is kept constant as the bias and modulation voltages are varied. Since the objective is to assess the extent to which SPM and optimized modulation increase the allowable transmission distance, fiber lengths of 100–150 km are considered. SPM leads to a considerable improvement in system performance for both maximum ER modulation and optimized modulation. Also, optimized modulation provides a significant improvement compared to maximum ER modulation. For a fiber length of 140 km, an average transmitted optical

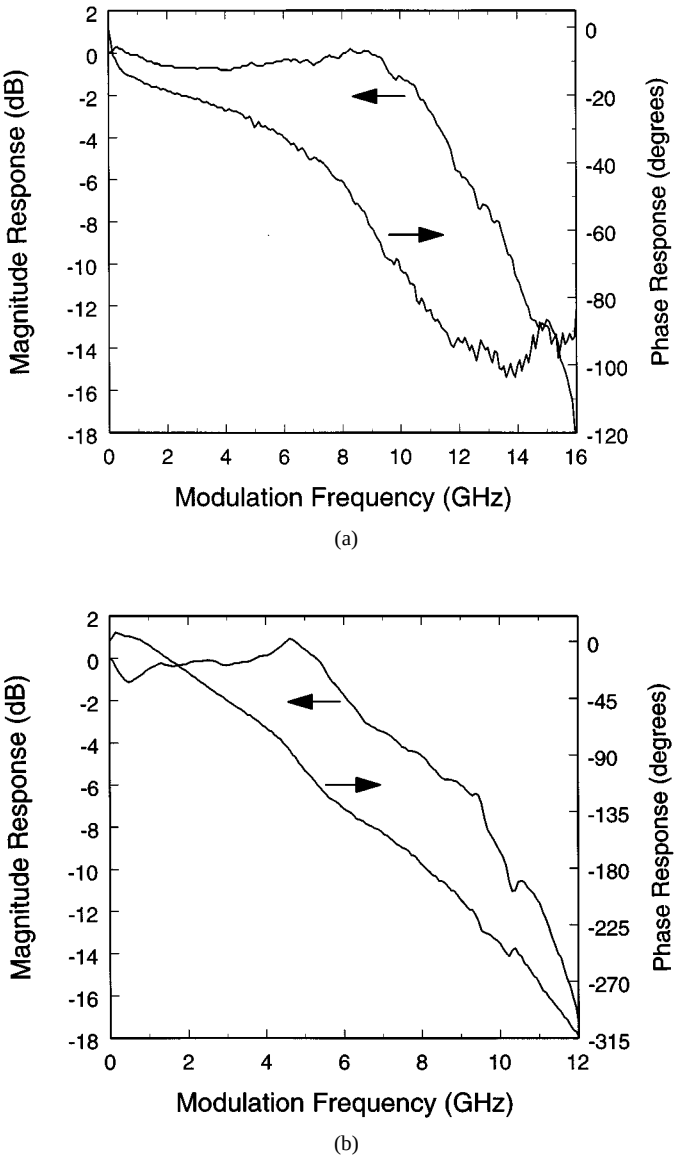

Fig. 6. Frequency response for: (a) the MQW Mach–Zehnder modulator and (b) the receiver.

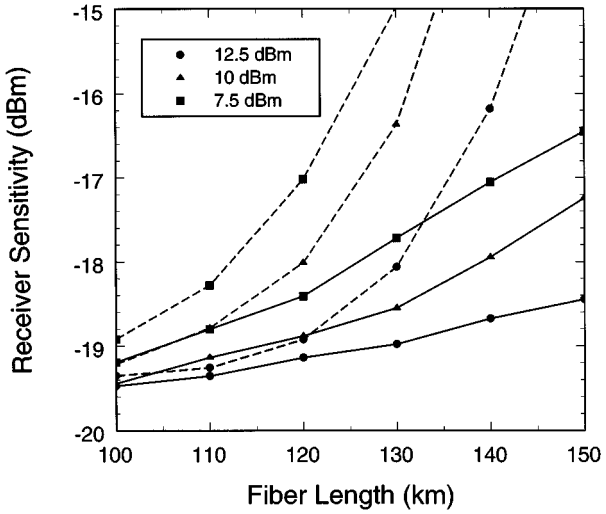

Fig. 7. Dependence of the receiver sensitivity on fiber length for a conventional modulator with a splitting ratio of 1. Results are presented for maximum extinction ratio modulation (dashed line) and optimized modulation (solid line) with average transmitted optical powers of 7.5, 10, and 12.5 dBm.

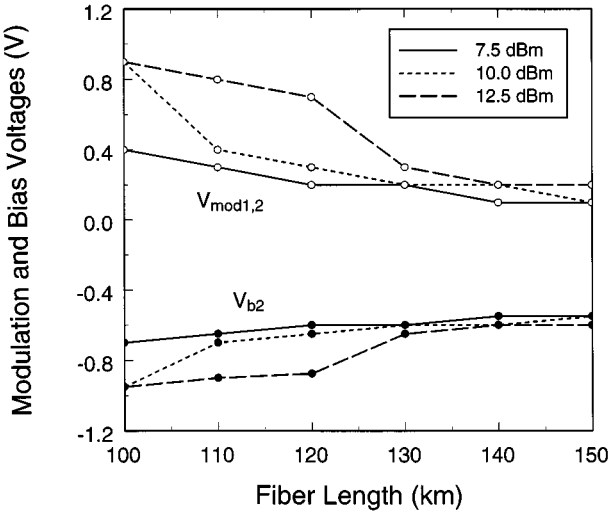

Fig. 8. Dependence of the optimum bias and modulation voltages on fiber length for a conventional modulator with a splitting ratio of 1. Results are presented for average transmitted optical powers of 7.5, 10, and 12.5 dBm. The optimum bias voltage for arm 1 is given by $V_{b1} = -4 - V_{b2}$.

power of 12.5 dBm, and optimized modulation, the penalty in receiver sensitivity relative to back-to-back performance is 1.5 dB. The extent of the improvements in system performance for average transmitted optical powers exceeding 12.5 dBm diminish. For a fiber length of 150 km and optimized modulation, the receiver sensitivity improves by 0.3 dB when the average transmitted optical power is increased from 12.5 to 15 dBm, and worsens by 1.2 dB when the power is increased to 17.5 dBm. If the transmitted power is too large, the combined phase modulation arising from the negative chirp property of the modulator and Kerr nonlinearity is excessive. The optimum bias and modulation voltages which correspond to the results in Fig. 7 are shown in Fig. 8. For fiber lengths of 130–150 km, the optimum bias and modulation voltages are quite similar for different values of the average transmitted optical power. The optimum modulation voltage decreases and the bias point moves toward the off-state as the fiber length increases. From Figs. 4 and 5, the modulator operates in a region of negative chirp with a high extinction ratio.

The results presented in Fig. 7 indicate the degradation in receiver sensitivity with increasing fiber length for a p-i-n-based receiver. While this clearly indicates the dispersion penalties, in some cases (e.g., average transmitted optical power of 5 dBm, maximum extinction ratio modulation) the system performance is attenuation limited rather than dispersion limited. This can be remedied by using an optically preamplified receiver. However, since the improvement in system performance obtained by combining SPM and optimum modulation conditions is being considered, the results for an average transmitted optical power of 12.5 dBm are of greatest interest. In this case, the sensitivity provided by a p-i-n based receiver is adequate for the results presented in Fig. 7, and for those that follow. Consequently, a preamplifier is not needed and would likely not be used in practice.

For comparison, results which correspond to those in Fig. 7 are presented in Fig. 9 for an optically preamplified receiver.

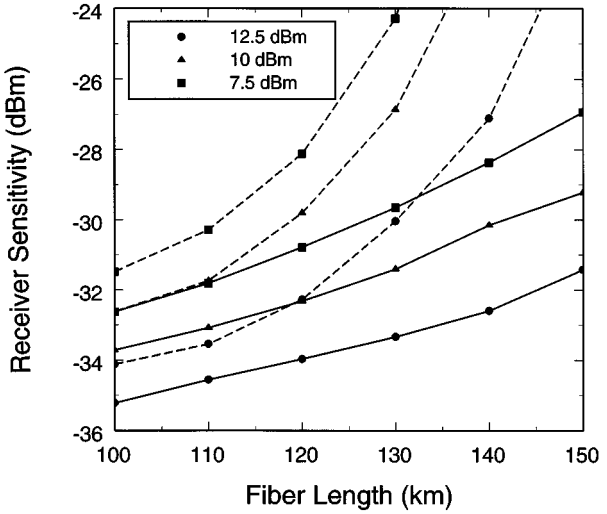

Fig. 9. Dependence of the receiver sensitivity on fiber length for a conventional modulator with a splitting ratio of 1 and an optically preamplified receiver. Results are presented for maximum extinction ratio modulation (dashed line) and optimized modulation (solid line) with average transmitted optical powers of 7.5, 10, and 12.5 dBm.

Relative to the back-to-back performance, the receiver sensitivity worsens more so with increasing fiber length for a preamplified receiver as the dominate source of noise is the signal-spontaneous beat noise. The comments made regarding the results in Fig. 7 also apply to the results of Fig. 9.

Fig. 10 illustrates the dependence of the receiver sensitivity on fiber length for a conventional modulator with a splitting ratio of 0.75. Asymmetric Y-branches improve the transmission performance for both maximum ER modulation and optimized modulation, and reduce the dependence of the transmission performance on the average transmitted optical power. For long fiber lengths, the optimized modulation yields a significant improvement over maximum ER modulation. For a fiber length of 150 km and optimized modulation, the receiver sensitivity is essentially unchanged when the average transmitted optical

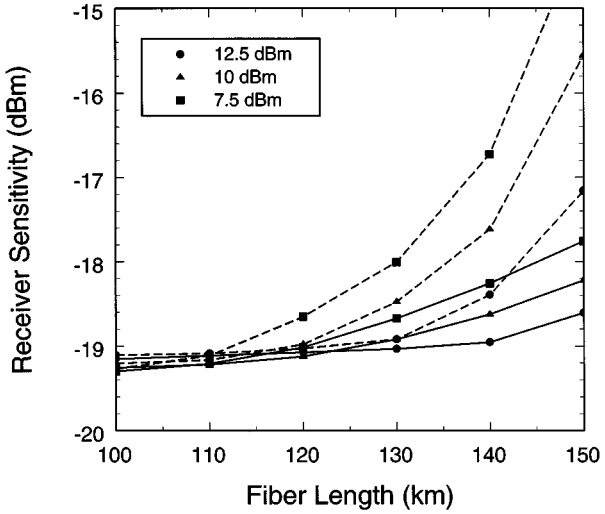

Fig. 10. Dependence of the receiver sensitivity on fiber length for a conventional modulator with a splitting ratio of 0.75. Results are presented for maximum extinction ratio modulation (dashed line) and optimized modulation (solid line) with average transmitted optical powers of 7.5, 10, and 12.5 dBm.

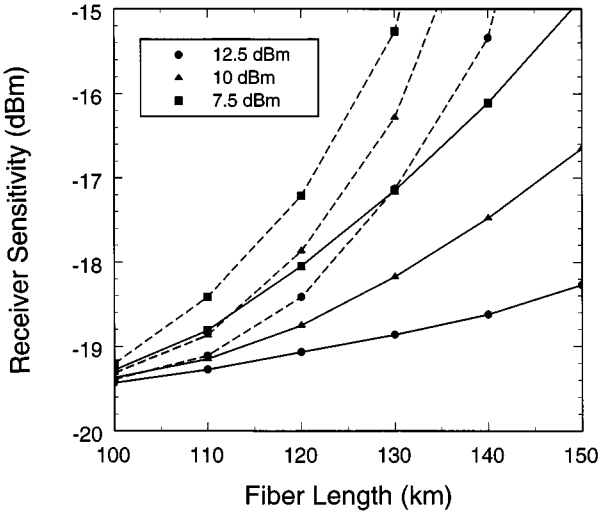

Fig. 12. Dependence of the receiver sensitivity on fiber length for a π phase-shift modulator with a splitting ratio of 1. Results are presented for maximum extinction ratio modulation (dashed line) and optimized modulation (solid line) with average transmitted optical powers of 7.5, 10, and 12.5 dBm.

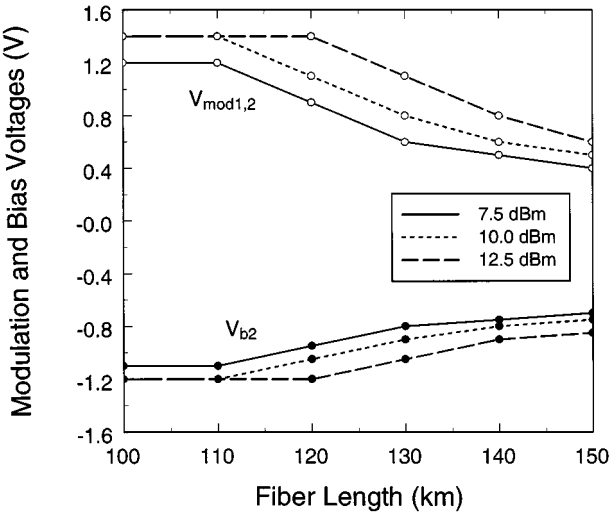

Fig. 11. Dependence of the optimum bias and modulation voltages on fiber length for a conventional modulator with a splitting ratio of 0.75. Results are presented for average transmitted optical powers of 7.5, 10, and 12.5 dBm. The optimum bias voltage for arm 1 is given by $V_{b1} = -4 - V_{b2}$.

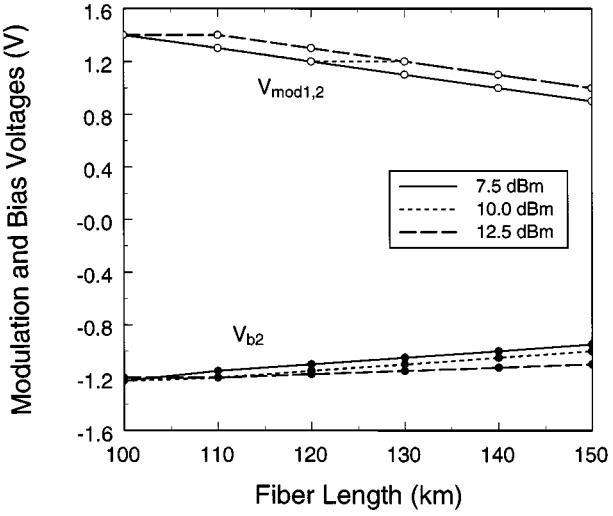

Fig. 13. Dependence of the optimum bias and modulation voltages on fiber length for a π phase-shift modulator with a splitting ratio of 1. Results are presented for average transmitted optical powers of 7.5, 10, and 12.5 dBm. The optimum bias voltage for arm 1 is given by $V_{b1} = -4 - V_{b2}$.

power is increased from 12.5 to 15 dBm. The optimum bias and modulation voltages shown in Fig. 11 exhibit the same trend as the results in Fig. 8. Compared to the conventional modulator with a splitting ratio of 1, the optimum modulation voltages are generally larger. Since the modulator has a negative α-parameter over the entire transmission curve, the modulation voltage is not constrained to a region of negative chirp as is the case for a splitting ratio of 1.

For a π phase-shift modulator and a splitting ratio of 1.3, the dependence of the receiver sensitivity on fiber length is shown in Fig. 14. For this modulator, the system performance exhibits a weak dependence on the average transmitted optical power. The advantage of the asymmetric Y-branch splitting ratios and the π phase-shift design are clearly evident (compare Figs. 7, 10, 12, and 14). As indicated in Section I, the π phase-shift modulator with asymmetric Y-branch waveguides is the result of efforts to optimize the device structure within the context of extending the system reach. Consequently, the phase modulation arising from the Kerr nonlinearity is of limited benefit. Indeed, for maximum ER modulation, an average transmitted power of 12.5 dBm does not yield the best system performance. Also, for a fiber length of 150 km and optimized modulation, the receiver sensitivity worsens by 0.2 dB when the average transmitted optical power is increased from 12.5 to 15 dBm. For maximum ER modulation and an average transmitted optical power of 7.5 dBm, the π phase-shift modulator with a splitting ratio of 1.3 offers better performance than a conventional modulator with a splitting ratio of 0.75. For average transmitted optical powers of 10 and 12.5

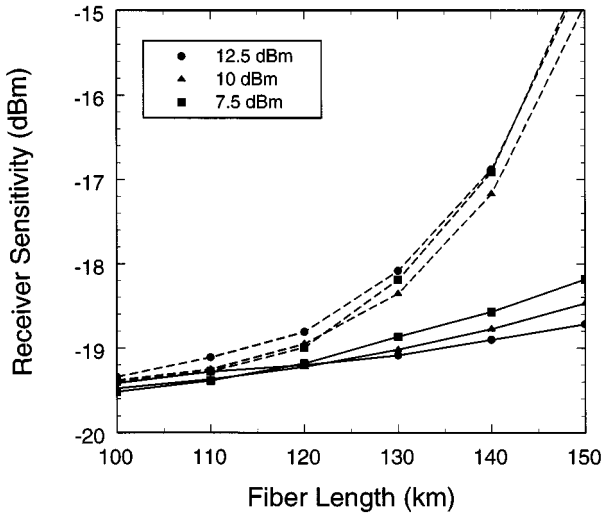

Fig. 14. Dependence of the receiver sensitivity on fiber length for a π phase-shift modulator with a splitting ratio of 1.3. Results are presented for maximum extinction ratio modulation (dashed line) and optimized modulation (solid line) with average transmitted optical powers of 7.5, 10, and 12.5 dBm.

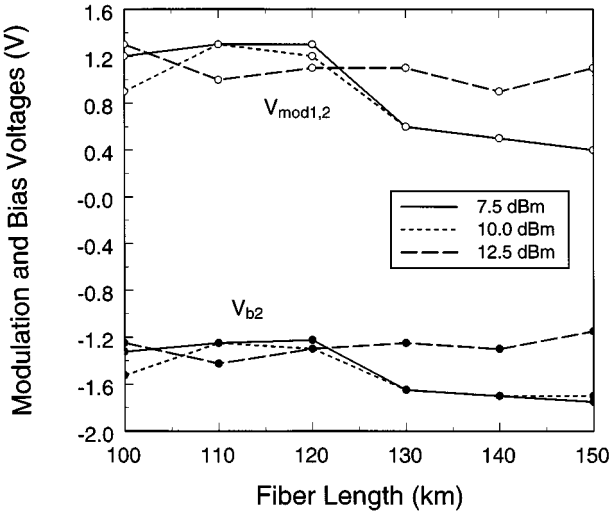

Fig. 15. Dependence of the optimum bias and modulation voltages on fiber length for a π phase-shift modulator with a splitting ratio of 1.3. Results are presented for average transmitted optical powers of 7.5, 10, and 12.5 dBm. The optimum bias voltage for arm 1 is given by $V_{b1} = -4 - V_{b2}$.

dBm, the conventional modulator exhibits better performance. With optimized modulation, the π phase-shift modulator with a splitting ratio of 1.3 offers some improvement compared to the conventional modulator with a splitting ratio of 0.75. The difference between the performance of the two modulators decreases to a negligible amount as the average transmitted optical power increases. The optimum bias and modulation voltages corresponding to the results in Fig. 14 are shown in Fig. 15. Compared to the other three modulators, the trend for the optimum modulation voltage to decrease and the bias point to move toward the off-state as the fiber length increases is not as pronounced or consistent for the different average transmitted optical powers. As above, this is attributed to the optimized device structure; a larger modulation voltage yields an appropriate amount of negative chirp.

Fig. 16 illustrates the dependence of the receiver sensitivity on the modulation voltage for a fiber length of 140 km and three values of the average transmitted optical power. For each value of the modulation voltage, the bias voltage has been optimized to yield the best receiver sensitivity. These results are also shown in the figure. As the average transmitted optical power is increased, the curves change from having two locally defined minima to having a broad range of voltages which provide near-optimum performance. A modulation voltage of 1.5 V corresponds to maximum ER modulation. The receiver sensitivity worsens for modulation voltages less than 0.3 V as the extinction ratio becomes quite small.

The dependence of the receiver sensitivity on fiber length for a π phase-shift modulator with a splitting ratio of 1 is shown in Fig. 12. A large variation with the average transmitted optical power and a significant improvement due to optimization of the bias and modulation voltages are observed. The results are comparable to those of the conventional modulator with a splitting ratio of 1, although the variation in system performance with the average transmitted optical power is smaller (larger) for maximum ER modulation (optimized modulation, respectively). For a fiber length of 150 km and optimized modulation, the receiver sensitivity improves by 0.4 dB when the average transmitted optical power is increased from 12.5 to 15 dBm. As illustrated in Fig. 13, the optimum bias and modulation voltages are remarkably similar for the different values of the average transmitted optical power and exhibit the same trends seen in Figs. 8 and 11. This similarity could be due to the high extinction ratio (ideally complete extinction) in the region where the α-parameter is largest, thereby reducing the dependence on the modulating voltage.The results in Figs. 7, 10, 12, and 14 generally depict a significant variation in system performance depending on the modulator design. Interestingly, an exception is the case of an average transmitted optical power of 12.5 dBm and optimized modulation. As summarized in Fig. 17, the receiver sensitivity varies by less than 0.5 dB for the four modulators over the range of fiber lengths 60–150 km. The variation is 0.3 dB for a fiber length of 140 km. For a fiber length of 140 km and maximum extinction ratio modulation, the corresponding variation in receiver sensitivity is 3.1 dB for an average transmitted optical power of 12.5 dBm, 4.5 dB for an average transmitted optical power of 10 dBm, and 6.6 dB for an average transmitted optical power of 7.5 dBm.

IV. Summary

The combined use of SPM and optimization of the bias and modulation voltages to increase the dispersion limited transmission distance of 10 Gb/s systems using nondispersion shifted optical fiber has been studied. Conventional and π phase-shift MQW Mach–Zehnder modulators with either symmetric or asymmetric Y-branch waveguides have been compared for the dual drive (push–pull) modulation format. Generally, the system performance depends rather strongly on

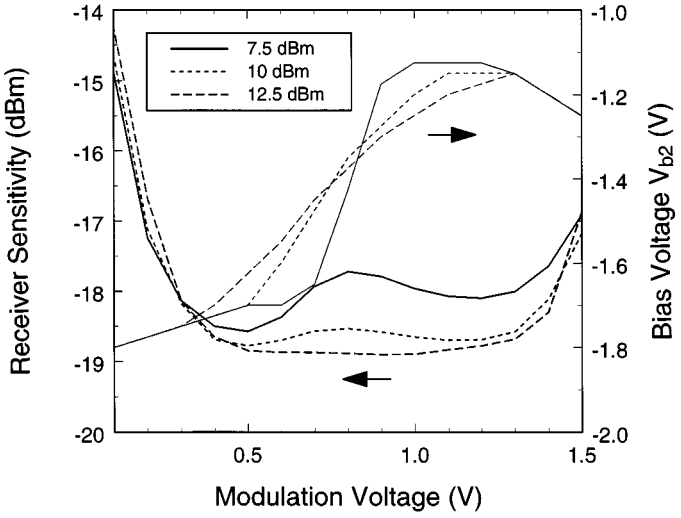

Fig. 16. Dependence of the receiver sensitivity and optimum bias voltage V_{b2} on modulation voltage for a π phase-shift modulator with a Y-branch splitting ratio of 1.3. The fiber length is 140 km. The optimum bias voltage for arm 1 is given by $V_{b1} = -4 - V_{b2}$.

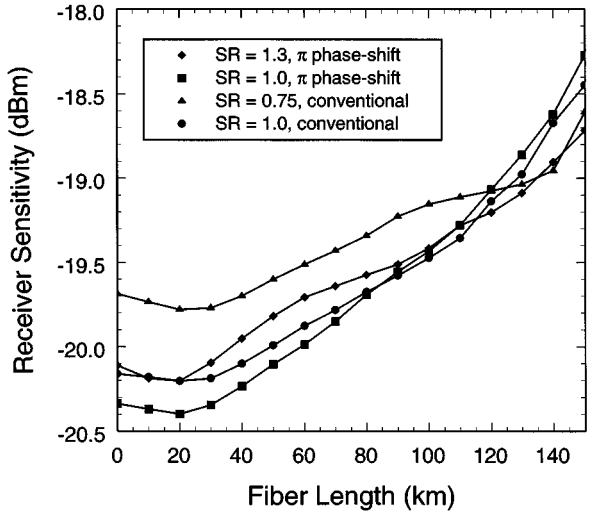

Fig. 17. Summary of results for the dependence of the receiver sensitivity on fiber length for the four modulators. Results are presented for optimized modulation and an average transmitted optical power of 12.5 dBm.

the modulator design, average transmitted optical power and modulation conditions. Modulators with asymmetric Y-branch waveguides offer improved system performance with a weaker dependence on the average transmitted optical power and modulation conditions. We observe, in particular, that the receiver sensitivities obtained for the four modulators considered in this paper vary, for fiber lengths from 60 up to 150 km, by less than 0.5 dB for an average transmitted optical power of 12.5 dBm and optimum modulation conditions. Hence the variation in system performance that might otherwise occur due to different modulator designs, or by inference to device-to-device variability of a particular design, can essentially be avoided. Given that the optimum bias and modulation voltages are rather weakly defined, the uniformity of system performance and device yield for maximum dispersion limited transmission can, therefore, be improved.

REFERENCES

[1] C. Rolland, R. S. Moore, F. Shepherd, and G. Hillier, "10 Gbit/s, 1.56 μm multiquantum well InP/InGaAsP Mach–Zehnder optical modulator," *Electron. Lett.*, vol. 29, pp. 471–472, 1993.

[2] C. Rolland, M. S. O'Sullivan, H. B. Kim, R. S. Moore, and G. Hillier, "10 Gb/s, 120 km normal fiber transmission experiment using a 1.56 μm multiquantum well InP/InGaAsP Mach–Zehnder modulator," in *Proc. Conf. Optical Fiber Commun.*, San Jose, CA, 1993, paper PD-27.

[3] J. C. Cartledge, C. Rolland, S. Lemerle, and A. Solheim, "Theoretical performance of 10 Gb/s lightwave systems using a III–V semiconductor Mach–Zehnder modulator," *IEEE Photon. Technol. Lett.*, vol. 6, pp. 282–284, 1994.

[4] D. M. Adams, C. Rolland, N. Puetz, R. S. Moore, F. R. Shepherd, H. B. Kim, and S. Bradshaw, "Mach–Zehnder modulator integrated with a gain-coupled DFB laser for 10 Gbit/s, 100 km NDSF transmission at 1.55 μm," *Electron. Lett.*, vol. 32, pp. 485–486, 1996.

[5] H. Sano, T. Ido, S. Tanaka, and H. Inoue, "10 Gb/s, 80 km normal fiber transmission by using multiple-quantum well Mach–Zehnder modulator," in *Optoelectron. Commun. Conf.*, Chiba, Japan, 1996, paper 17D2-4.

[6] P. Delansay, D. Penninckx, S. Artigaud, J.-G. Provost, J.-P. Hébert, E. Boucherez, J. Y. Emery, C. Fortin, and O. Le Gouezigou, "10 Gbit/s transmission over 90-127 km in the wavelength range 1530–1560 nm using an InP-based Mach–Zehnder modulator," *Electron. Lett.*, vol. 32, pp. 1820–1821, 1996.

[7] J. Yu, C. Rolland, A. Somani, S. Bradshaw, and D. Yevick, "Phase-engineered III–V MQW Mach–Zehnder modulators," *IEEE Photon. Technol. Lett.*, vol. 8, pp. 1018–1020, 1996.

[8] D. Penninckx, P. Delansay, E. Boucherez, C. Fortin, and O. Le Gouezigou, "InP/GaInAsP π-phase shifted Mach–Zehnder modulator for wavelength independent (1530–1560 nm) propagation performance at 10 Gbit/s over standard dispersive fiber," *Electron. Lett.*, vol. 33, pp. 697–698, 1997.

[9] D. Penninckx and P. Delansay, "Comparison of the propagation performance over standard dispersive fiber between InP-based π-phase-shifted and symmetrical Mach–Zehnder modulators," *IEEE Photon. Technol. Lett.*, vol. 9, pp. 1250–1252, 1997.

[10] C. Lawetz, J. C. Cartledge, C. Rolland, and J. Yu, "Modulation characteristics of semiconductor Mach–Zehnder optical modulators," *IEEE J. Lightwave Technol.*, vol. 15, pp. 697–703, 1997.

[11] P. Delansay, S. Gauchard, H. Helmers, D. Penninckx, S. Gurib, and F. Brillouet, "2.5 Gbit/s transmission over 1086 km of standard single-mode fiber using an integrated laser Mach–Zehnder modulator," in *Proc. Conf. Optical Fiber Commun.*, San Jose, CA, 1998, paper TuI7.

[12] C. Rolland, "InGaAsP-based Mach–Zehnder modulators for high-speed transmission systems," in *Proc. Conf. Optical Fiber Commun.*, San Jose, CA, 1998, paper ThH1.

[13] D. M. Adams, C. Rolland, A. Fekecs, D. McGhan, A. Somani, S. Bradshaw, M. Poirier, E. Dupont, E. Cremer, and K. Anderson, "1.55 μm transmission at 2.5 Gbit/s over 1102 km of NDSF using discrete and monolithically integrated InGaAsP/InP Mach–Zehnder modulator and DFB laser," *Electron. Lett.*, vol. 34, pp. 771–773, 1998.

[14] J. C. Cartledge and B. Christensen, "Optimum operating points for electroabsorption modulators in 10 Gb/s transmission systems using nondispersion shifted fiber," *J. Lightwave Technol.*, vol. 16, pp. 349–357, 1998.

[15] J. C. Cartledge, "Optimizing the bias and modulation voltages of MQW Mach–Zehnder modulators for 10 Gb/s transmission on nondispersion shifted fiber," *J. Lightwave Technol.*, vol. 17, pp. 1142–1151, 1999.

[16] J. Yu, "The beam propagation method and its application to the design of semiconductor modulators," Ph.D. dissertation, Queen's University, 1994.

[17] S. S. Walklin, "Multilevel signaling for increasing the capacity of high-speed optical communication systems," Ph.D. dissertation, University of Alberta, 1997.

[18] F. Koyama and K. Iga, "Frequency chirping in external modulators," *J. Lightwave Technol.*, vol. 6, pp. 87–93, 1988.

[19] J. C. Cartledge, "Transmission performance α-parameter for semiconductor Mach–Zehnder optical modulators," *J. Lightwave Technol.*, vol. 16, pp. 372–379, 1998.

J. C. Cartledge (S'74–M'79–SM'96) received the B.Sc. degree in mathematics and engineering in 1974 and the M.Sc. and Ph.D. degrees in mathematics from Queen's University, Kingston, ON, Canada, in 1976 and 1979, respectively.

From 1979 to 1982, he was a Member of the Scientific Staff at Bell-Northern Research, Ottawa, ON, Canada, where his work involved fiber-optic systems for the exchange access network and high-capacity digital radio systems. Since 1982, he has been with the Department of Electrical and Computer Engineering, Queen's University. He leads research projects sponsored by Communications and Information Technology Ontario and Photonics Research Ontario (two provincial centers of excellence) and by the Canadian Institute for Photonic Innovations (a federal center of excellence). He has spent one-year sabbatical leaves with the Lightwave Systems Technology Research Division of Bellcore, Red Bank, NJ, in 1988-1989, and with the Optical Communications Department of Tele Danmark Research, Hørsholm, Denmark, in 1995-1996. He has served as a consultant in the area of lightwave technology to several organizations. His research interests include semiconductor optical modulators, semiconductor lasers, optical amplifiers, and wavelength-division-multiplexed systems.

Dr. Cartledge served on the Technical Program Committee for the Conference on Optical Fiber Communications for the period 1994-1997, the Technical Program Committee for the joint meeting of the International Conference on Integrated Optics and Optical Fibre Communications and the European Conference on Optical Communications (IOOC/ECOC'97), the International Program Committee for the International Conference on Applications of Photonic Technology (1998 and 2000), and the Program Committee for the Ninth Canadian Semiconductor Technology Conference. He is a member of the Optical Society of America (OSA) and Professional Engineers Ontario.